Mine Water Environ (2012) 31:53–61
DOI 10.1007/s10230-012-0172-x

TECHNICAL ARTICLE

Electrical and Seismic Tomography Used to Image the Structure of a Tailings Pond at the Abandoned Kettara Mine, Morocco

Meriem Lghoul · Teresa Teixidó · José Antonio Peña · Rachid Hakkou · Azzouz Kchikach · Roger Guérin · Mohammed Jaffal · Lahcen Zouhri

Received: 14 October 2011 / Accepted: 26 January 2012 / Published online: 10 February 2012

Abstract The Kettara site (Morocco) is an abandoned pyrrhotite ore mine in a semi-arid environment. The site contains more than 3 million tons of mine waste that were deposited on the surface without concern for environmental consequences. Tailings were stockpiled in a pond, in a dyke, and in piles over an area of approximately 16 ha and have generated acid mine drainage (AMD) for more than 29 years. Geophysical methods have been used at the Kettara mine site to determine the nature of the geological substrate of the tailings pond, the internal structure of the mine wastes, and to investigate the pollution zones associated with sulphide waste dumps. Electrical resistivity tomography (ERT) and seismic refraction data were acquired, processed, and interpreted; the results from ERT and seismic refraction were complementary. A topographical survey of the tailings disposal area was also undertaken to estimate the volume of wastes and quantify the AMD process. Two-dimensional inverse models were used to investigate the geophysical data and indicated alteration zones at depth. It was determined that the material could be classified into three categories: tailings, with low resistivity (5–15 Ω m) and low velocity (500–1,800 m/s); altered, black shales, with intermediate resistivity (20–60 Ω m) and velocity (2,000–3,500 m/s), and; materials with high resistivity and velocity (>60 Ω m and >4,000 m/s, respectively), including unaltered shales associated with quartzite seams. The low-resistivity zone generates AMD, which migrates downward through fractures and microfractures. The substrate is composed of broken and altered shale, which facilitates AMD infiltration.

Keywords Acid mine drainage (AMD) · Mine waste · Electrical resistivity tomography (ETR) · Kettara mine site · Seismic refraction tomography

M. Lghoul · A. Kchikach · M. Jaffal
Equipe de recherche E2G, Cadi Ayyad University (UCAM), BP 549, 40000 Marrakech, Morocco

M. Lghoul · R. Hakkou (✉)
IDRC (Canada) Research Chair in Management and Stabilization of Mining and Industrial Wastes, LCME, Cadi Ayyad University (UCAM), Marrakech, Morocco
e-mail: rhakkou@fstg-marrakech.ac.ma; hakou@yahoo.com

M. Lghoul · R. Guérin
UMR 7619 Sisyphe, Univ Pierre and Marie Curie-Paris 6, Case 105, 4 Place Jussieu, 75252 Paris Cedex 05, France

T. Teixidó · J. A. Peña
Instituto Andaluz de Geofísica, Univ de Granada, Granada, Spain

L. Zouhri
Institut Polytechnique La Salle Beauvais, Beauvais, France

Introduction

Geophysical methods are increasingly being used with great success to delineate areas contaminated with potentially harmful elements and compounds, including acidic seepage at industrial landfills and mine waste sites. These methods have also been used to define the petrophysical properties and internal structure of tailings impoundments and waste rock piles (Buselli and Lu 2001; Campbell and Fitterman 2000; Chouteau et al. 2005; Guérin et al. 2004; Martin-Crespo et al. 2010; Martinez-Pagán et al. 2009; Placencia-Gòmez et al. 2010; Poisson et al. 2009; Rucker et al. 2009; Shemang et al. 2003; Sjodahl et al. 2005; Vanhala et al. 2005). To monitor or decontaminate affected sites, a complete knowledge of their geology and

hydrogeology is necessary, as is knowledge of the behaviour of the pollutants and their means and routes of transport. Geophysical methods are very useful in providing this information (Guérin et al. 2004) and can be a cost-effective alternative to expensive drilling and sampling programs in engineering, geological, and hydrogeological applications (Nasab et al. 2011). Geophysics can be applied with great value to generate information about the subsurface over a large area in a reasonable time frame and in a cost-effective manner (Burger et al. 2006).

Mine wastes containing metallic sulphides commonly generate acid mine drainage (AMD). There are many physical, geochemical, and biological processes that lead to the production of AMD; these have been summarized elsewhere (e.g. Evangelou 1995; Kleinmann et al. 1981; Singer and Stumm 1970). The site-specific reactions are largely dictated by internal structure and the physical and chemical properties of the mine wastes (Ramalho et al. 2009).

However, direct observation by drilling and excavation of trenches can be difficult due to the heterogeneous nature of the materials. Moreover, the information obtained is localized and the destructive nature of drilling disturb the structure of materials and can be a source of pollution. Under these conditions, geophysical methods offer a relatively low cost alternative for characterizing the internal structure of the tailings and determining the extent of AMD migration. Geophysical methods are nondestructive in nature and are simple to implement, compared to drilling. The characterisation of contaminated sites using geophysical methods is essential for the successful design of remediation strategies.

The Marrakech area (Fig. 1a) is one of the principal metallogenic provinces of Morocco. Several mine sites there are either being exploited or are currently abandoned. The present study relates to the abandoned Kettara mine, which is representative of the Marrakech area; it generates significant AMD and a rehabilitation project has been initiated.

The rehabilitation scenario being investigated at the Kettara mine involves using fine alkaline phosphate waste (APW) as both an amendment and a 'store and release' (SR) cover (Hakkou et al. 2009). This process will require that all of the Kettara coarse tailings be collected and placed over the old tailings pond. The coarse tailings would be amended with approximately 20 cm of APW. Then, an APW capillary barrier would be placed over the Kettara mine waste; in the semi-arid climate, this barrier is expected to limit infiltration of water to the reactive mine wastes, thus reducing AMD production (Hakkou et al. 2009). To facilitate the success of this rehabilitation project, it was important to determine the nature of the geological substrate of the tailings pond and the internal structure of the mine wastes, and to estimate the volume of tailings by determining the thickness of the tailings layer in the tailings pond.

Site Description

Geological Setting

The central Jebilet metapelites (Sarhlef schists) outcrop a few kilometres north of Marrakech in a wide area corresponding to the central unit of the Hercynian Jebilet massif. The Sarhlef schists are derived from Middle to Upper Visean shales deposited in an anoxic platform and are affected by a very-low-to low-grade metamorphism contemporaneous with a post-Visean shortening. Deformation and metamorphic gradients are observed towards the major shear zones, and there are numerous intrusions present in the unit (Huvelin 1977). Sulphide deposits in the studied area are generally located close to the intrusions. These ore bodies are organised into subvertical lineaments concurrently with the regional schistosity.

The Kettara sulphide deposit is a typical example of a metamorphosed deposit hosted by Visean volcano-sedimentary formations. The tectonic and microtectonic structures observed in the neighbourhoods of the principal surface of the tailings correspond to strike-slip faults with quartzo-carbonated seams and micro-fractures with quartzitic seams, and schistosity, which affects all of the black shale formation (Lghoul et al. 2012).

Kettara Mine

The abandoned Kettara pyrrhotite ore mine, exploited by the SYPEK corporation, is located approximately 30 km north–north–west of the town of Marrakech in the core of the central Jebilet Mountains (Fig. 1a). The mining village of Kettara and the mining infrastructure are located downstream from the tailings pond area (Fig. 1b). According to the latest statistics (2004), the population of Kettara is approximately 2,000. The climate is classified as semi-arid with a mean annual rainfall of approximately 250 mm. Rainfall can occur over short periods and with high intensity. The annual potential evaporation typically exceeds 2,500 mm. From 1964 to 1981, the mine produced more than 5.2 million metric tons (Mt) of pyrrhotite concentrate containing an average of 29% wt sulphide. Pyrrhotite was extracted from the ore by gravimetric separation (jigs). This ore enrichment process generated a wide range of particle size fractions in the tailings (jigs refuse materials). Although ore reserves were still abundant, the mine was closed in June 1982 due to difficulties encountered during pyrrhotite concentrate production.

The tailings can be divided into two broad classes of material; coarse tailings (fine gravel) were deposited on the 15 m high dyke and in 1 m high tailings piles, while fine tailings (silt) were deposited in the tailings pond (Fig. 1d). The Kettara wastes contain 1.6–14.5 wt% sulphur, mainly

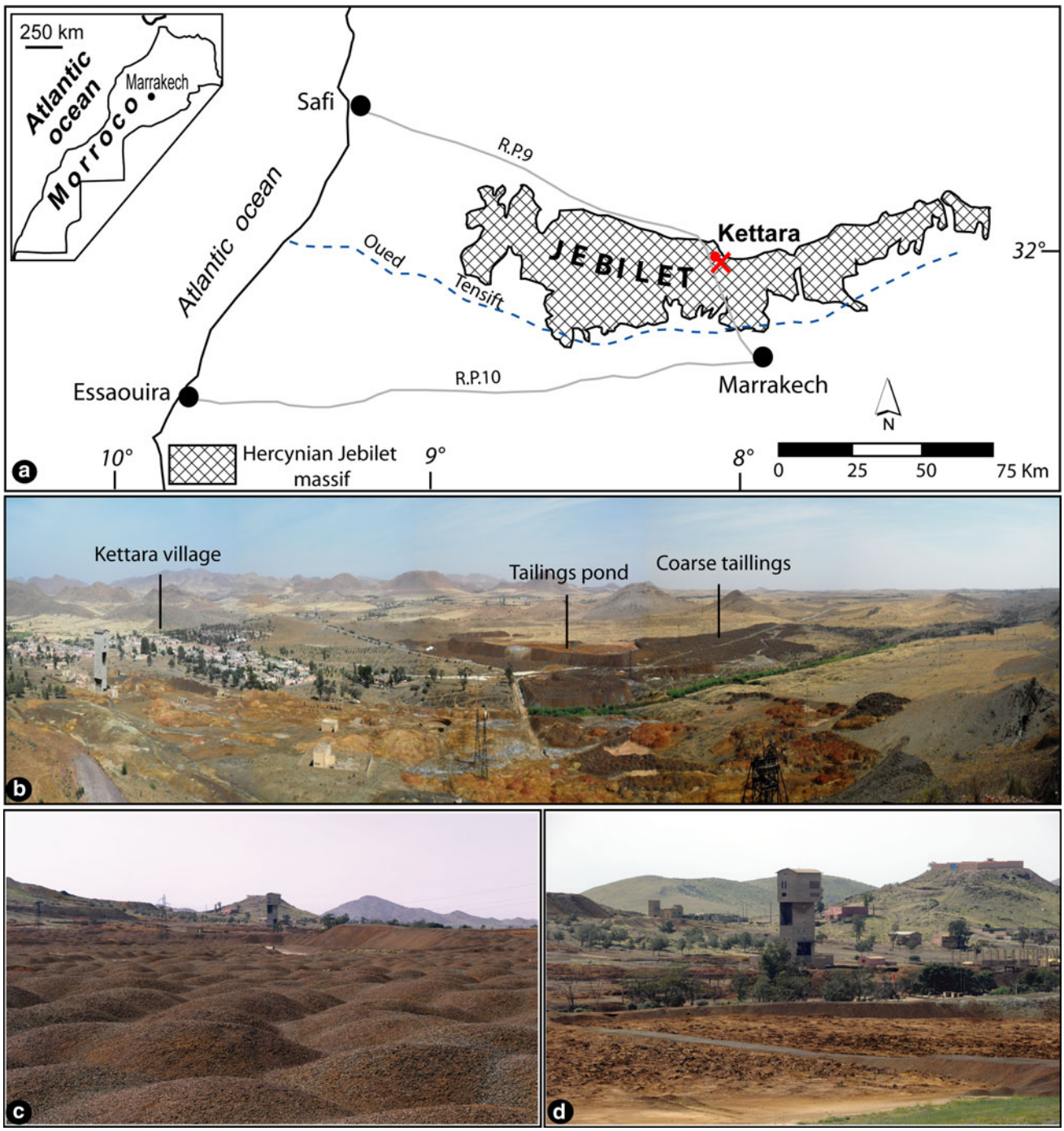

Fig. 1 The study area: **a** a panoramic view, and photos, **b** illustrating the proximity of the village to the mine waste area and the serious AMD problem, **c** the coarse tailings, and **d** the tailings pond

as sulphide minerals (e.g., pyrrhotite, pyrite, chalcopyrite, galena, and sphalerite) (Hakkou et al. 2008a). Because of their larger particle size and greater permeability, facilitating exposure to oxygen and the percolation of water, the pollution potential of the coarse tailings in Kettara is much greater than that of the fine tailings. The Kettara mine tailings produced significant amounts of AMD. Effluent water samples had low pH (2.9–4.2) and elevated concentrations of sulphate (from 47 to 5,000 mg/L) and iron (from 1 to 1,200 mg/L). Concentrations of Cu and Zn reached 58 and 45 mg/L, respectively (Hakkou et al. 2008b). The Kettara tailings piles and pond will continue to release acid for a long time. Several secondary minerals have been observed at the surface of the mine site. These

minerals occur as extremely fine-grained particles or as a continuous precipitate layer known as hardpan. Additional precipitates occur in other forms, such as 'blooms' or efflorescent salts. The presence of these minerals in large quantities shows that AMD generation is still very active at Kettara.

The substrate is composed of broken shale, which could facilitate AMD infiltration. Furthermore, the principal groundwater table is located in this formation, at a depth between 10 and 20 m. Groundwater sampled from wells downstream of the mining wastes is contaminated by the AMD, mainly by sulphates (>1,200 mg/L) and have high conductivity values (3,000–3,680 μS/cm) (Lghoul et al. 2012). Understanding the processes that control the extent and dispersion of contaminants away from the abandoned mines could help reduce adverse effects at active mining sites (Cidu et al. 2011). This study focused on the Kettara tailings pond (Fig. 2), where geophysical methods were used to investigate the pollution zones associated with sulphide waste dumps.

The tailings pond is surrounded by dry coarse tailings (Figs. 1c and 2), which are distributed over the shale soil. It was impossible to acquire either an electric profile or a seismic profile of these materials (gravels) because they connect poorly with electrodes and provide unsatisfactory emplacement of geophones. So, to quantify these coarse tailings, a GPS (differential) topographical survey was conducted during the last week of October 2010.

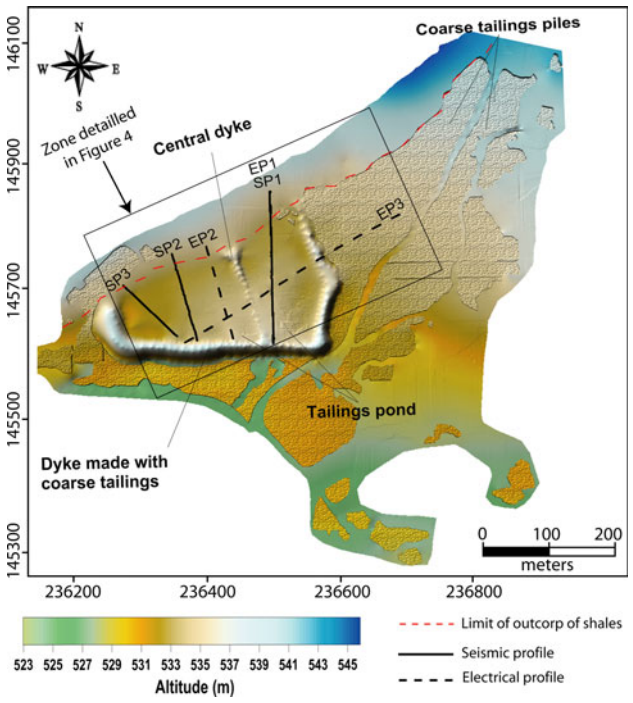

Fig. 2 A 3-D view of the topographical survey. This survey was acquired with differential GPS. The map shows the locations of the acquired profiles (three electrical profiles and three seismic profiles). The coarse tailings piles were topographically mapped using a basic unit 'relief grid'. For more information, see the text

Methods

GPS Topographical Survey

A topographical survey was conducted over the surface of the fine tailings dam and in its surroundings to characterise the coarse tailings (Fig. 2); we also measured the co-ordinates of all of the geophysical profiles. For this work, we employed a pair of geodetic GPS receivers, bifrequence-differential models Zmax (Thales), using real-time kinematic (RTK) differentials.

To map the coarse tailings, we delineated their contours and then used the geometrical similarity of this area to determine a square area of significance. We mapped this area in detail and used it as a basic unit "relief grid," extending it to all of the sectors affected by the coarse tailings. Thus, we calculated the volume of all of the coarse tailings at 94,320 m^3.

Electrical Survey

Electrical resistivity tomography (ERT) is a geophysical technique that involves placing a series of electrodes along a straight line (for 2-D acquisition). To measure ground resistivity, two electrodes inject direct current into the subsurface and then the electric potential is measured between them with two other electrodes. This procedure must be repeated along the profile by moving the four electrodes. The investigation depth is determined by separating the electrodes using different distances along the profile. The electrical equipment read these measurements automatically.

The flow of the current injected at the surface by the electrodes is affected by the electrical properties of the materials. This relationship is influenced by lithology, texture, the presence of fluid or empty pore space. In the present study, the electrical resistivity of the materials is modified by the AMD content, which decreases the resistivity (by increasing the electrical conductivity).

ERT was used to provide a continuous cover along the SP profiles (Fig. 3) to get quantitative information about their geo-electric properties. A 2-D resistivity tomography profile was obtained using the Terrameter Lund Imaging System (ABEM Instruments) using a 64 electrode array. A Schlumberger configuration was used with a compromise unit electrode spacing of 2 m in the central part of the profile and 5 m near the border to obtain information for a thickness of 25–30 m with suitable precision. We chose a sigma (typical deviation) of 0.1% for the data acquisition and a weighting of 4 samplings.

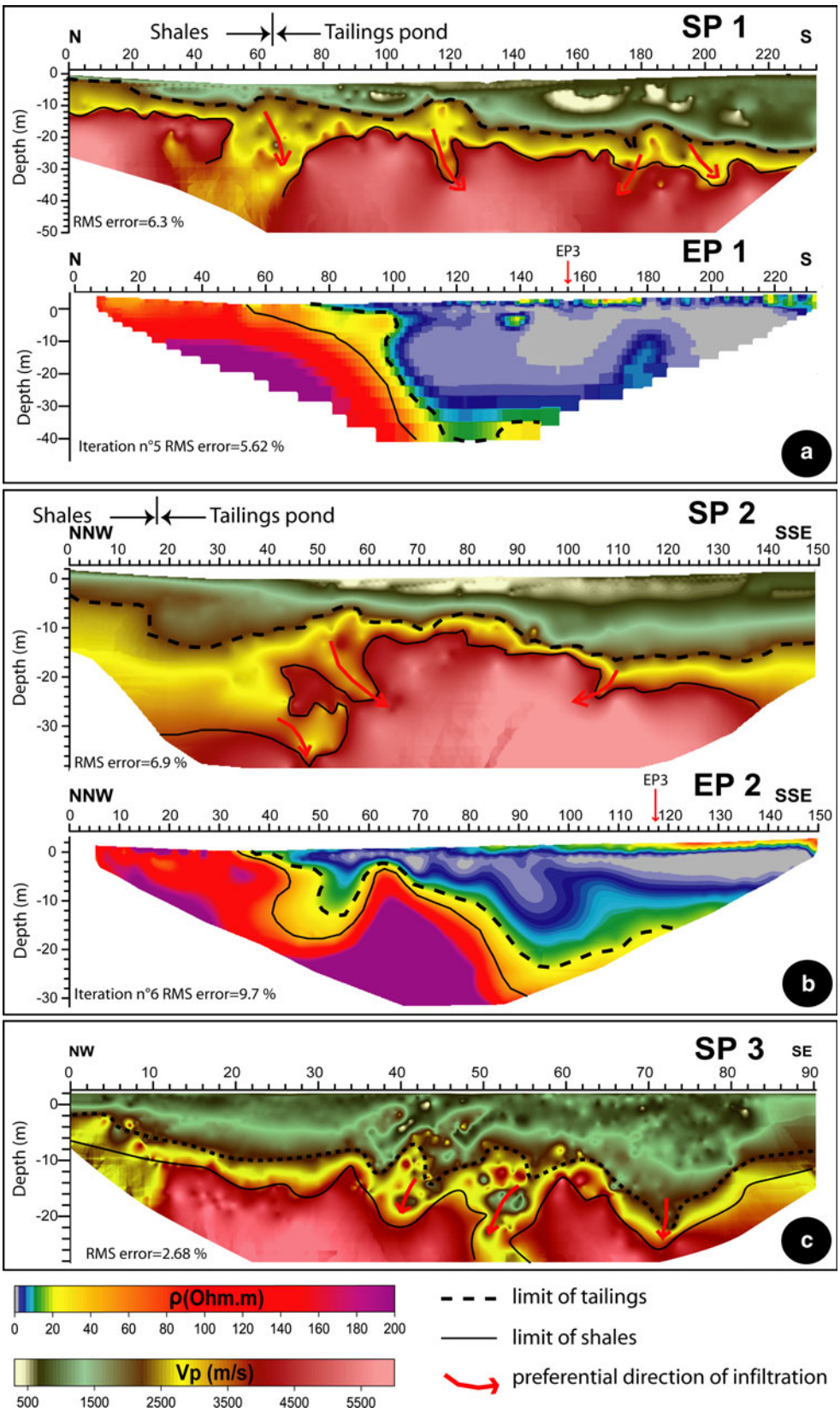

Fig. 3 Interpretations of **a** the seismic profile SP1 combined with the electrical profile EP1, **b** the seismic profile SP2 combined with the electrical profile EP2, and **c** the seismic profile SP3

The data collected are called apparent resistivities because they are influenced by the resistivities of all of the layers that the current has crossed. To determine apparent resistivities, we must calculate the real resistivities of the ground. ERT data must be inverted to produce detailed electrical structures of the cross-sections below the survey lines; these are classically presented as pseudo-sections. These measured pseudo-sections include topographic variations for processing with a 2-D inverse modeling technique, and to give the estimated true resistivities.

Schematically, the subsurface is divided into a grid in which each cell is assigned a resistivity value. Usually, the initial model is an average of the apparent resistivities from the field data (experimental apparent resistivity). Through this initial model, we calculate the apparent resistivities (calculated apparent resistivity), and the difference between the experimental apparent resistivities allows for the modification of the cell resistivity (real resistivity) values and for the generation of a second 2-D model; the iterative process continues until the differences between the apparent calculated and apparent experimental resistivities (% RMS) are minimal.

The ERT data were inverted using the software package Res2DInv (Geotomo Software, possessed by Instituto Andaluz de Geofisica, Granada, Spain). The inversion process used in this forward modeling program is based on the robust-constrained least-squares method (Loke and Barker 1996). This produces a model that emphasizes the vertical resistivity features, because in the geological context, sharp interfaces between the different units are expected. We choose the following inversion options: (a) a model refinement that allows us to get model cells with a width equal to half the unit electrode spacing. This helps to obtain more accurate results when large resistivity changes are expected near the ground surface, (b) a maximum number of iterations, equal to 9, for the inversion process, The ERT data were also processed and interpreted by geophysicists of the Laboratory of Applied Geophysics, University and Polytechnic Institute of Lasalle-Beavais, France). The results converge with those resulting from inversion made in Granada. For the all profiles, the root mean square (RMS) error was less than 10%.

Seismic Survey

Seismic refraction tomography is a geophysical method that generates and records elastic refraction waves from the ground boundaries; these layers reflect changes in the mechanical properties of strata at the Earth's surface. The current practice is to employ a seismic source (in this case, an 8 kg hammer) and to record the wave-front propagation over the terrain surface through an array of receivers. In most cases, the geophones are placed at a fixed distance from one another, and a predetermined number of shots (hammer strikes) should be taken along the survey. We set off shots at 10 m intervals along realized seismic profiles. Our field data were acquired with a Stratavisor (Nz-24, Geometrics Inc.) seismograph with an array of 48 geophones.

Seismic profiles were constructed on the same days, and in close proximity, to the ERT profiles. Their lengths ranged from 115 to 235 m with geophones spaced at distances of 3 and 5 m. Profiles SP1 and EP1 (Fig. 2) were coincident so that we could correlate the two geophysical responses.

For each shot, a seismic register was created to record the arrival times of the waves at each geophone. We calculated the velocities of the propagation waves based on the geometry of the sensor array. The seismic velocities were affected by the mechanical properties, the lithology, and the extent of compaction of the materials. In the present study, the seismic response did not allow us to delineate the boundary between the tailings and substrate, due to comparable compactness between the two, but we were able to identify velocity variations within the tailings and the substrate, which we attributed to preferred zones of AMD circulation.

The seismic refraction tomography method is based on the timing of P-refraction waves and results in P-velocity models (2-D). The geophysical inversion process begins with calculating all times for all ray-paths starting from a shoot point and ending at the geophones. These rays record mechanical information of the entire path; therefore, this information must be sorted and assigned to the corresponding subsurface location. This sorting is achieved with specific inversion algorithms [wavepath Eikonal travel time (WET) tomography processing; Lecomte et al. 2000]. Similar to the electric inversion schema, the subsurface is divided into a grid in which each cell is assigned one velocity value. In most cases, the initial model is an average of the velocity ray-paths. The first stage is to calculate the arrival times of each ray, i.e., the time corresponding to each shot-geophone pair. Second, these calculated times are compared with the experimental times, and their difference is used to modify the velocity values in each cell, and then generate a second 2-D model. This iterative process continues until the differences between the apparent calculated and apparent experimental resistivities (% RMS) are minimal. We used RayFract (V 3.18, Intelligent Resources Inc.) code for the processing of this seismic data.

Results and Discussion

Seismic profiles have been proposed as a means to distinguish the basement morphology of shales because the

lithology of the basement is more compact than the tailings. The black or altered shales investigated in this study had resistivity values between ~60 and 500 Ω m, which varied due to the presence or absence of quartzite seams. These resistivities are regarded as an upper limit to distinguish the uncontaminated shales.

To correlate the electrical and seismic geophysical responses of the materials present in the study area, we ensured that the seismic profile SP1 coincided with the electrical profile EP1 and that the electrical profile EP2 was parallel with SP2 (Fig. 2).

The section profile EP1 shows a low resistivity zone (<15 Ω m) beginning at a distance of 75 m, which reflects the tailings ponds. This zone can reach a depth of more than 40 m at the core of the dam. This suggests that tailings were stockpiled in a large pit located to the east of the tailings pond. At the 100 m distance, towards the initial extreme of the profile, the resistivity increased significantly, with values higher than 80 Ω m (Fig. 3a). This transition occurred gradually and in a vertical direction. The boundary with a yellow-orange colour corresponds to the top of the altered or black shales. The high resistivities of the shales may be explained by the presence of quartz seams. Two boundaries are defined: the limit of the mine tailings (at 15 Ω m) and the top of the shales (60 Ω m).

The SP1 seismic profile also shows three layers. The first layer has an average velocity between 350 and 2,000 m/s, with a thickness ranging from 8 m in the north to 20 m in the extreme south. This layer corresponds to the tailings pond deposits. The second interpreted layer has a velocity between 2,000 and 3,800 m/s, with an irregular morphology, and corresponds to the altered shales. Below this layer, there is a third layer with a velocity average of 4,000 m/s, corresponding to the shales. The transition towards the shales is described by an increase in velocity in a narrow horizon (Fig. 3a). The two defined boundaries: the limit of the tailings (1,800 m/s) and the limit of the shales (3,800 m/s).

The obtained pseudo-section of the EP2 profile shows low resistivity (15 Ω m) values starting at a distance of 40 m. This profile corresponds to the materials affected by AMD; the depth of this effect expands for 20 m at a distance between 84 and 104 m (Fig. 3b). A resistant body is located at a distance between 62 and 64 m, which divides two polluted zones: a great area towards the centre-south of the tailings pond and a small area towards the north. The high resistivity area corresponds to the fresh shales. The irregular boundary between high and low resistivity indicates the top of altered shales (the limit of the tailings).

Three horizons were also interpreted in the SP2 seismic model. The first horizon, with an average velocity ranging between 350 and 2,000 m/s and a thickness between 5 and 18 m, is composed of tailing pond deposits. Between a distance of 52 and 90 m, a layer with a very low velocity (<500 m/s) was detected, which corresponds to the much altered tailings pond at the surface. The following seismic horizon has an average velocity of 3,000 m/s and corresponds to the altered shales. As demonstrated in profile SP1, the transition between the altered and unaltered shales is very well defined, especially towards the northern part of the study area. The third layer corresponds to the almost unaltered shales, with an average velocity of 3,800 m/s (the limit of the shales).

The SP3 seismic profile also shows three layers (Fig. 3c); the first layer has an average velocity between 350 and 2,000 m/s. This layer has an irregular morphology and corresponds to the tailings pond deposits. The second interpreted layer has a velocity between 2,000 and 3,800 m/s and corresponds to the altered shales. Below this layer, there is a third layer with a velocity average of 4,000 m/s, corresponding to the unaltered shales. The tailings substrate (indicated by arrows) clearly act as preferred flow zones for the AMD.

In this study, the geophysical methods used highlighted the following points: the electrical resistivity of the tailings (<20 Ω m) is definitely different from the shale substrate (>80 Ω m). This was also confirmed by the previous study (Lghoul et al. 2012). Since, in this context, the resistivity is primarily related to the electrolytes, we think that this boundary between the tailings and substrate is most realistic. The boundary provided by the seismic method does not always coincide with that given by ERT; we think that cementation of the lower part of tailings conferred compactness comparable with that of the higher altered part of the substrate, which makes it difficult to use the method to differentiate the two materials. However, the highlighted seismic zones with low velocities should correspond to the more altered zones of the tailings and are rooted in the substrate (Fig. 3 SP1, SP2, and SP3). These are zones which could constitute preferred paths of AMD circulation. The fractures and N50°-oriented micro-fractures apparently act as preferential drains of leachates, and so these micro-fractures are being eroded and altered by the leachates (Lghoul et al. 2012). Underground flow would be preferentially directed along these structures.

The resistivity and seismic velocity increase from the top to the bottom of the tailings pond and correspond to the compaction of this material. The high values in resistivity and seismic velocity of the shales correspond to the presence of quartzite seams.

Figure 4 shows the three electric profiles and the two seismic profiles located in the western part of the study area. In these schematic models, three major layers were defined for each profile: the first layer corresponds to altered materials (tailings pond), the second corresponds to the altered shales and the third corresponds to the unaltered

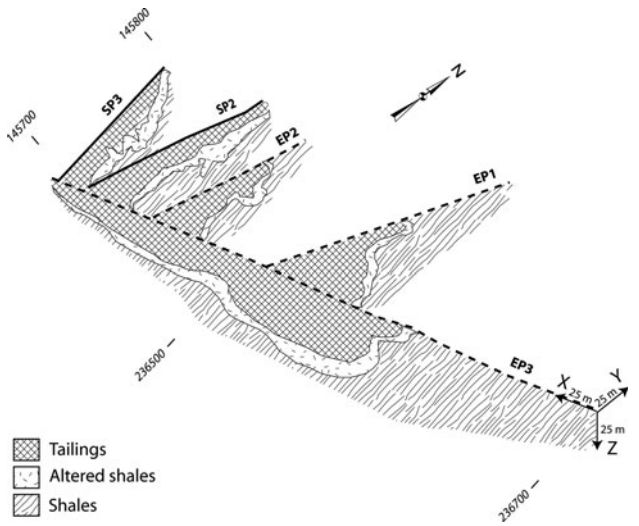

Fig. 4 A 3-D synthetic model of the acquired profiles; three layers were identified: the first corresponds to the affected materials, the second to the altered *black shales*, and the last to the unaltered shales. These layers are bounded by the limit of the tailings and the top of the shales

shales. The electric profiles describe two major zones of the expansion of leachate present on both sides of the central dyke.

The waste volumes calculated using the 2-D geophysical models coupled with relatively little geological data may have led to an initial overestimation of waste volumes (Chambers et al. 2005). Moreover, the resistivity model provides only an approximate guide to the subsurface resistivity distribution, due to the smoothing and averaging effects and the decreased resolution with depth inherent in the smoothness-constraint inversion technique.

We have considered, in calculating the volume of wastes, the ERT-defined boundary between the tailings and the precise topographical measurements made at the surface. Isosurfaces were used to define waste volumes with resistivities below 15 Ω m. The 15 Ω m contour fell at a depth broadly corresponding to the estimated depth to bedrock indicated by the resistivity model and site investigation data. The volume of the western area tailings pond is estimated at 176,200 m^3. The estimated volume of the eastern area tailings is substantially greater, at 286,200 m^3.

The oxidation of 1,341,000 t (the specific gravity of the tailings is 2.9) of fine tailings containing 4 wt% of sulphide sulphur will release more than 161,000 t of sulphates. This high sulphate load may be critically detrimental to the local water resources. The average sulphate production rate of fine tailings is very high: 2,000–8,000 mg SO_4/kg/week (Hakkou et al. 2008b). This suggests that fine tailings will continue to release acid and sulphates for a long time. According to the geophysical interpretation, infiltration should preferentially flow towards the altered shales, particularly in the north. The most important infiltration zone is located to the west of the central dyke.

Conclusion

The electrical tomography data showed close agreement in the physical properties of the area and the presence of conductive zones and their characteristics. The seismic refraction data, though better suited to stratigraphic environments, complemented the other geophysical information.

Additionally, using seismic refraction, we imaged the structure of the underlying subsoil and leakage pathways in the bedrock that could work as AMD conduits. These results show that joint use of these geophysical methods can be successfully employed to provide a better understanding of how geological features develop at depth and to estimate the extent of AMD. They also allowed us to categorize the materials into three categories. The first category corresponds to the tailings, which have low resistivity (5–15 Ω m) in the electric profiles and low velocity (500–1,800 m/s) in the seismic profiles. The second layer corresponds to the altered, black shales, which have intermediate resistivity (20–60 Ω m) and velocity (2,000–3,800 m/s). The last category, with high resistivity and velocity (>60 Ω m and >4,000 m/s, respectively) corresponds to the unaltered shales associated with quartzite seams.

The tailings pond contains 1,780,000 t of wastes, which will release more than 280,000 tons of sulphate. AMD generation will continue for decades or centuries if no remedial actions are taken. The broken and altered shales will facilitate AMD infiltration.

This work reveals that joint use of geophysical techniques enables a complete environmental characterisation of mine sludge structures, allowing the monitoring and estimation of potential pollution. Geophysical results will also help locate where best to drill to confirm the depth of tailings.

Acknowledgments This work was supported through the International Research Chairs Initiative, a program funded by the International Development Research Centre, and by the Canada Research Chairs program, Canada. The authors also thank the AECI (Agencia Española de Cooperación Internacional, Ref. A/025780/09) and Comités Mixtes Interuniversitaires Franco-Marocaine (Action Intégrée n°MA/09/209) for their financial and technical support.

References

Burger HR, Sheehan AF, Jones CH (2006) Introduction to applied geophysics: exploring the shallow subsurface. WW Norton and Company, New York City

Buselli G, Lu K (2001) Groundwater contamination monitoring with multichannel electrical and electromagnetic methods. J Appl Geophys 48:11–23

Campbell DL, Fitterman DV (2000) Geoelectrical methods for investigating mine dumps. In: Proceedings of 5th international conference on acid rock drainage (ICARD), Soc for Mining, Metallurgy and Exploration, Littleton CO, USA, pp 1513–1523

Chambers JE, Meldrum PI, Ogilvy RD, Wilkinson PB (2005) Characterization of a NAPL-contaminated former quarry site using electrical impedance tomography. Near Surf Geophys 3:79–90

Chouteau M, Poisson J, Aubertin M, Campos D (2005) Internal structure and preferential flow of a waste rock pile from geophysical surveys. In: Proceedings of symp for the application of geophysics to environmental and engineering problems (SAGEEP), pp 289–297

Cidu R, Frau F, Da Pelo S (2011) Drainage at abandoned mining sites: natural attenuation of contaminants under different seasons. Mine Water Environ 30:113–126

Evangelou VP (1995) Pyrite oxidation and its control. CRC Press, Boca Raton

Guérin R, Bégassat P, Benderitter Y, David J, Tabagh A, Thiry M (2004) Geophysical study of the industrial waste land in Mortagne-du-Nord (France) using electrical resistivity. Near Surf Geophys 3:137–143

Hakkou R, Benzaazoua M, Bussière B (2008a) Acid mine drainage at the abandoned Kettara mine (Morocco). 1. Environmental characterization. Mine Water Environ 27:145–159

Hakkou R, Benzaazoua M, Bussière B (2008b) Acid mine drainage at the abandoned Kettara mine (Morocco). 2. Mine waste geochemical behavior. Mine Water Environ 27:160–170

Hakkou R, Benzaazoua M, Bussière B (2009) Laboratory evaluation of the use of alkaline phosphate wastes for the control of acidic mine drainage. Mine Water Environ 28:206–218

Huvelin P (1977) Etude géologique et gîtologique du massif hercynien des Jebiletes (Maroc occidentale). Notes et Mémoires du Service Géologique du Maroc, 232 bis, p 307

Kleinmann RLP, Crerar DA, Pacelli RR (1981) Biogeochemistry of acid mine drainage and a method to control acid formation. Mining Eng 79:300–305

Lecomte I, Gjoystdal H, Dahle A, Pedersen OC (2000) Improving modeling and inversion in refraction seismics with a 1rst-order Eikonal solver. Geophys Prospect 48:437–454

Lghoul M, Kchikach A, Hakkou R, Zouhri L, Guerin R, Bendjoudi H, Teíxido T, Penã JA, Enriqué L, Jaffal M, Hanich L (2012) Etude géophysique et hydrogéologique du site minier abandonné de Kettara (région de Marrakech, Maroc): contribution au projet de réhabilitation. Hydrolog Sci J 57:1–12

Loke MH, Barker RD (1996) Rapid least squares inversion of apparent resistivity pseudosections by a quasi-Newton method. Geophys Prospect 44:131–152

Martín-Crespo T, De Ignacio-San JoseC, Gòmez-Ortiz D, Martín-Velázquez S, Lillo-Ramos J (2010) Monitoring study of the mine pond reclamation of Mina Concepciòn, Iberian Pyrite Belt (Spain). Environ Earth Sci 59:1275–1284

Martínez-Pagán P, Faz-Cano A, Aracil E, Arocena JM (2009) Electrical resistivity imaging revealed the spatial properties of mine tailing ponds in the Sierra Minera of southeast Spain. J Environ Eng Geophys 14:63–76

Nasab N, Hojat A, Kamkar-Rouhani A, Javar HA, Maknooni S (2011) Successful use of geoelectrical surveys in Area 3 of the Gol-e-Gohar iron ore mine, Iran. Mine Water Environ 30:208–213

Placencia-Gòmez E, Parviainen A, Hokkanen T, Loukola-Ruskeeniemi K (2010) Integrated geophysical and geochemical study on AMD generation at the Haveri Au–Cu mine tailings, SW Finland. Environ Earth Sci 61:1435–1447

Poisson J, Chouteau M, Aubertin M, Campos D (2009) Geophysical experiments to image the shallow internal structure and the moisture distribution of a mine waste rock pile. J Appl Geophys 67:179–192

Ramalho E, Carvalho J, Barbara S, Monteiro Santos F (2009) Using geophysical methods to characterize an abandoned uranium mining site, Portugal. J Appl Geophys 67:14–33

Rucker DF, Glaser DR, Osborne T, Maehl WC (2009) Electrical resistivity characterization of a reclaimed gold mine to delineate acid rock drainage pathways. Mine Water Environ 28:146–157

Shemang EM, Laletsang K, Chaoka TR (2003) Geophysical investigation of the effect of acid mine drainage on the soil and groundwater near a mine dump, Selebi-Phikwe Cu-Ni Mine, NE Botswana. In: Proceedings of SAGEEP, pp 930–937

Singer PC, Stumm W (1970) Acidic mine drainage: the rate determining step. Science 167:1121–1123

Sjödahl P, Dahlin T, Johansson S (2005) Using resistivity measurements for dam safety evaluation at Enemossen tailings dam in southern Sweden. Environ Geol 49:267–273

Vanhala H, Räisänen ML, Suppala I, Huotari T, Valjus T, Lehtimäki J (2005) Geophysical characterizing of tailings impoundment: a case from the closed Hammaslahti Cu–Zn mine, eastern Finland. Geological Survey of Finland, Current Research (2003–2004), special paper 38, pp 49–60